HHS Public Access

Author manuscript

J Immunol. Author manuscript; available in PMC 2020 February 01.

Published in final edited form as:

J Immunol. 2019 February 01; 202(3): 991–1002. doi:10.4049/jimmunol.1800736.

Transthyretin Stimulates Tumor Growth through Regulation of Tumor, Immune and Endothelial Cells

Chih-Chun Lee[#*], **Xinchun Ding**[#*], **Ting Zhao**[*], **Lingyan Wu**[*], **Susan Perkins**[†], **Hong Du**[*], and **Cong Yan**[*]

[*] Department of Pathology and Laboratory Medicine, Indiana University School of Medicine, Indianapolis, IN

[†] Department of Biostatistics, Indiana University School of Medicine, Indianapolis, IN

[#] These authors contributed equally to this work.

Abstract

Early detection of lung cancer offers an important opportunity to decrease mortality while it is still treatable and curable. Thirteen secretory proteins that are Stat3 downstream gene products were identified as a panel of biomarkers for lung cancer detection in human sera. This panel of biomarkers potentially differentiates different types of lung cancer for classification. Among them, the transthyretin (TTR) concentration was highly increased in human serum of lung cancer patients. TTR concentration was also induced in the serum, bronchoalveolar lavage fluid, alveolar type II epithelial cells and alveolar myeloid cells of the CCSP-rtTA/$(tetO)_7$-Stat3C lung tumor mouse model. Recombinant TTR stimulated lung tumor cell proliferation and growth, which were mediated by activation of mitogenic and oncogenic molecules. TTR possesses cytokine functions to stimulate myeloid cell differentiation, which are known to play roles in tumor environment. Further analyses showed that TTR treatment enhanced the reactive oxygen species (ROS) production in myeloid cells and enabled them to become functional myeloid derived suppressive cells. TTR demonstrated a great influence on a wide spectrum of endothelial cell functions to control tumor and immune cell migration and infiltration. TTR-treated endothelial cells suppressed T cell proliferation. Taken together, these 13 Stat3 downstream inducible secretory protein biomarkers potentially can be used for lung cancer diagnosis, classification, and as clinical targets for lung cancer personalized treatment if their expression levels are increased in a given lung cancer patient in the blood.

Introduction

Lung cancer is a very aggressive malignant form of cancer, and is one of the biggest public health challenges facing the United States and many other countries. Although incidence rates have been stabilized, an estimated 154,050 Americans are expected to die from lung cancer in 2018, accounting for approximately 25.3 percent of all cancer deaths (https://

Address correspondence to: Dr. Cong Yan, Department of Pathology and Laboratory Medicine, Indiana University School of Medicine, 975 W Walnut Street, IB424G, Indianapolis, IN 46202. Tel: 1-317-278-6005. coyan@iupui.edu; or Dr. Hong Du, Department of Pathology and Laboratory Medicine, Indiana University School of Medicine, 975 W Walnut Street, IB424E, Indianapolis, IN 46202. Tel: 1-317-274-6535. hongdu@iupui.edu.

www.cancer.org/cancer/non-small-cell-lung-cancer/about/key-statistics.html). According to World Health Organization, around 1.37 million people die from lung cancer each year worldwide (http://www.who.int/mediacentre/factsheets/fs297/en/). Lung cancer is by far the leading cause of cancer death among both men and women. Each year, more people die of lung cancer than of colon, breast, and prostate cancers combined. Lung cancer is a difficult disease to detect in its early stages, with greater than 50% of patients diagnosed with lung cancer presenting with metastatic disease (http://seer.cancer.gov/statfacts/html/lungb.html). Early detection of lung cancer is an important opportunity for decreasing mortality while it is still treatable and curable (1). The overall 5-year survival rate is ~15 percent. Thus, it is essential to better understand the mechanisms that initiate lung carcinogenesis and find easy-use biomarkers for more accurate lung cancer detection. Due to heterogeneity of lung cancers, a panel of biomarkers should be used for more accurate lung cancer detection and classification.

Signal transducer and activator of transcription 3 (Stat3) is well known for its lung cancer-promoting activity (2) (3) (4). The Stat3 expression level was up-regulated in human lung cancers (5). To assess the consequences of STAT3 persistent activation in the lung, a doxycycline-controlled CCSP-rtTA/$(tetO)_7$-Stat3C bitransgenic mouse model was generated that over-expresses STAT3C (a constitutively active form of STAT3) in alveolar type II (AT II) epithelial cells. In sequential steps, Stat3C over-expression up-regulated pro-inflammatory molecules, increased inflammatory cell infiltration and caused adenocarcinomas in the lung (2). The GeneChip microarray analysis of lung tumor from the CCSP-rtTA/$(tetO)_7$Stat3C mice revealed around 800 up- and down-regulated genes as potential lung cancer biomarkers with at least two-fold expression changes ($p<0.05$) (2). Since most of these genes are intracellular proteins, it is inconvenient to use them for the purpose of clinical diagnosis without going through biopsy.

Here we report identification of 13 soluble and secretory proteins, which were selected from the Stat3 downstream gene list with 2-fold increase ($p<0.05$) in lung tumors, as a panel of biomarkers for lung cancer detection in humans using the sera. This panel of biomarkers can potentially be used to differentiate different types of lung cancers. To elucidate tumorigenic functions of these biomarkers, one of 13 protein biomarkers, transthyretin (TTR), was selected for further analysis for its role in lung cancer promotion. TTR (also called prealbumin) is a homotetramer plasma protein of ~55 kDa, which is known for the transportation of thyroxine and retinol through binding to retinol-binding protein (6). However, TTR null mice suggest that TTR is not essential to thyroid hormone metabolism (7) and may not be crucial on retinol metabolism (8). We demonstrated that recombinant TTR protein enhanced myeloid cell differentiation, altered angiogenesis, and promoted lung tumor cell proliferation *in vitro* and tumor growth *in vivo*.

Materials and Methods

Human sample

The human serum samples of normal subjects and lung cancer patients (adenocarcinomas patients, squamous cell carcinomas patients, and small cell lung cancer patients) were

obtained from the Biosample Repository Core Facility (BRCF) of Fox Chase Cancer Center in Philadelphia.

Animal and cell lines

All scientific protocols involving the use of animals have been approved by the Institutional Animal Care and Use Committee (IACUC) in Indiana University School of Medicine and followed guidelines established by the Panel on Euthanasia of the American Veterinary Medical Association. Animals were housed under IACUC-approved conditions in a secure animal facility in Indiana University School of Medicine. Protocols involving the use of recombinant DNA or biohazardous materials have been approved by the Biosafety Committee of Indiana University School of Medicine and followed guidelines established by the National Institute of Health. The generation of doxycycline-controllable and alveolar type II epithelial cell-specific CCSP-rtTA/$(tetO)_7$-Stat3C bitransgenic mouse model was previously described (2). Lewis lung carcinoma (LLC) cells or B16 melanoma cells were purchased from the American Type Culture Collection (ATCC).

Antibody production

The purified full length TTR protein was used as the antigen for rabbit immunization by a custom antibody production service (Rockland Immunochemicals Inc. Limerick, PA). The quality and the titer of TTR antibody in the serum was determined by ELISA and Western blotting.

Molecular cloning of the mouse TTR cDNA and Induction of recombinant TTR protein

The RNAs were extracted from mouse myeloid HD1A cells (Applied Biological Materials Inc., Canada) using RNeasy kit (QIAGEN) and reversely transcribed into cDNA by oligo-dT primer using Thermoscript transcriptase (Invitrogen, Carlsbad, CA) according to the manufacturer's instruction. The cDNA was used in the polymerase chain reaction (PCR) to amplify TTR amplicon by Phusion DNA polymerase (New England Biolabs, Ipswich, MA) using primers Xma I-TTR-F (5'- AGC CCC GGG TGC CAC CAT GGC TTC CCT TCG ACT CTT C −3') and Not I-FLAG-TTR-R (5'- ACA GCT CAG AGC GGC CGC TCA CTT GTC ATC GTC ATC CTT GTA ATC ATT CTG GGG GTT GCT GAC GA −3'). The TTR amplicon (502 bp) was gel-purified and digested with Xma I and Not I restriction enzymes (New England Biolabs) and cloned into the pGEX-4T-1 expression vector (GE Healthcare Life Sciences, Pittsburgh, PA). A thrombin-specific cleavage site was present between GST and inserted TTR-Flag. The reading frame and the inserted TTR-Flag cDNA was confirmed by sequencing and named as pGEX-4T-TTR-Flag. The expression of GST-TTR-Flag fusion protein (~42 kDa) was induced by IPTG in BL21 E. coli and the protein samples collected from pre-induction, pellet, and supernatant were analyzed by SDS-PAGE and visualized by Coomassie blue staining. The GST-TTR-Flag fusion protein in the soluble fraction was purified by GST column and digested by thrombin. The TTR-Flag band (~17 kDa) was monitored by Coomassie staining and confirmed by Western blot analyses using anti-FLAG antibody. The purified recombinant TTR-Flag protein was subjected to lipopolysaccharide (LPS) removal by endotoxin removal column.

Western blot analysis

Bronchoalveolar lavage fluid (BALF) and serum were collected from wild-type, doxycycline-treated or untreated CCSP-rtTA/$(TetO)_7$-Stat3C bitransgenic mice. Serum (1 μl) or BALF (6 μl) was mixed with Laemmli sample buffer (Bio-Rad, Hercules, CA) and heated at 95°C for 5 min, fractioned in Novex® 4–20% Tris-Glycine Mini Gels (Invitrogen, Carlsbad, CA) and transferred to polyvinylidene difluoride membranes (Bio-Rad, Hercules, CA). The membranes were incubated with rabbit-anti-TTR antibody (Abbiotec, San Diego, CA) at 4°C overnight and followed with secondary antibody (horseradish peroxidase (HRP)-conjugated goat-anti-rabbit IgG, 1:2000). TTR was detected by incubation with SuperSignal West Pico chemiluminescent substrate (Thermo Scientific) and the images were taken by ChemiDoc MP imaging system (Bio-Rad).

To determine activation of signaling pathways by TTR treatment, LLC cells were seeded in 6-well plates until ~75% confluent, and treated with LPS-removed TTR (1 and 0.1 μM) for 2 hrs in the presence of exotoxin inhibitor polymyxin B (PMB) (100 μg/mL). The treated LLC cells were harvested using Cellytic-M cell lysis buffer with phosphatase and protease inhibitors. The cell lysates were centrifuged to remove insoluble cell debris. Protein concentrations in the lysates were determined by the BCA method. Twenty microgram total protein was analyzed by SDS-PAGE and transferred to a PVDF membrane. The membranes were probed by various antibodies (1:1000) against p-mTOR, p-NF-κB p65, p-S6, p-Stat3, p-ERK, p-Akt and p-p38 (Cell Signaling Technology, Danvers, MA), followed by secondary anti-rabbit IgG, HRP-conjugated antibody (1:2000).

Immunohistochemistry staining of TTR

The lungs from doxycycline-treated or untreated CCSP-rtTA/$(TetO)_7$-Stat3C mice were inflated with 4% paraformaldehyde, harvested, stored in 4% paraformaldehyde overnight and paraffin embedded as previously described (9). Tissue sections (5-μM) were incubated with rabbit-anti-TTR antibody (1:500) at 4°C overnight, and followed by biotinylated goat-anti-rabbit antibody (1:1,000). The color signals were detected with a Vectastain Elite ABC kit following manufacturer's instructions (Vector Laboratory, Burlingame, CA). Rabbit IgG was used as negative control.

The proliferation of tumor cells in vitro assay

Mouse B16 melanoma cells and LLC cells were seeded in 48-well plates (5×10^3 cells/well). After overnight incubation, cells were treated with 0, 1 or 5 μM LPS-removed TTR in the presence of 100 μg/mL PMB. After 2 or 3 days, tumor cells were detached by accutase (Sigma, St. Louis, MO) and the cell numbers were counted by a hemocytometer.

Subcutaneous injection of tumor cells in mouse models

LLC cells (5×10^5) or B16 melanoma cells (2×10^5) were incubated with 20 μM TTR/PMB protein for 1 hr and subcutaneously flank-injected into syngeneic C57BL/6 mice. Furthermore, LLC cells (5×10^5) or B16 melanoma cells (1×10^6) incubated with 20 μM TTR/PMB were subcutaneously flank-injected into allogeneic FVB/N mice. The tumor growth was estimated by measuring the maximal length (L) and width (W) and the tumor volume was calculated using the formula of $0.5xLxW^2$ (mm^3).

siRNA knockdown

LLC cells grown in 60-mm dish until ~70% confluence were transfected with three siRNAs (against three independent regions) targeting Akt, mTOR, Akt/mTOR or NFκB p65 using Dharmacon siRNA transfection reagent according to the manufacturer's instructions (Dharmacon, Lafayette, CO). After 2-day incubation, LLC cells (5×10^5 cells) were harvested and treated with 5 μM TTR/PMB and subcutaneously flank-injected into wild-type C57BL/6 mice for tumor growth analyses. The effectiveness of siRNA knockdown was assessed by Western blot of each target protein.

Fluorescence activated cell sorting (FACS) analysis

For *in vivo* immune cell profiling, TTR (320 μg / mouse) was i.v. injected into wild type mice twice a week for two weeks, and PBS was used as control. Single-cell suspensions from the bone marrow, blood and spleen were prepared as previously described (10). Approximately 1–3 × 10^6 cells from various organs were incubated with FcR blocking Abs in FACS buffer (BD BioSiences, San Jose, CA) followed by isotype control or surface specific primary Abs. For *in vitro* differentiation, the bone marrow cells from wild type mouse were cultured in 96 wells plate (1× 10^6 cells per well), and treated with LPS-removed TTR/PMB at concentrations of 0, 0.2, 1 or 5 μM for 2 days. Cells were harvested for surface staining with fluorescence conjugated anti-mouse antibodies. Anti-mouse MHCII FITC, anti-mouse Ly6C FITC, anti-mouse CD11c PE, anti-mouse F4/80 Apc, anti-mouse CD11b, anti-mouse Ly6G (RB6–8c5), anti-mouse CD4 FITC, anti-mouse CD8 PE, and anti-mouse B220 Apc were purchased from e-Biosciences (San Diego, CA).

For TTR expression in mice, cells from the lung, blood, and spleen were prepared and stained with surface markers (SP-C, Ly6G and CD11b antibodies). Fixed cells were permeabilized using BD Cytofix/CytopermTM Fixation/Permeabilization Kit according to the manufacture's instruction. Cells were incubated with the anti-TTR antibody (1:500) at 4°C overnight. Next day, cells were washed and labeled with the secondary antibody for flow cytometry analysis. For expression of signaling molecules in bone marrow cells or ECs, cells were treated with 50 μg/mL PMB or 1 μM TTR/PMB for 2 hours and then stained with various cell surface markers, followed by intracellular staining of anti-mouse pAKT, anti-mouse pmTOR, anti-mouse pS6, anti-mouse pp38, anti-mouse pERK and anti-mouse pp65 antibodies (Cell signaling, Beverly, MA). Flow cytometry was analyzed on a LSRII machine (BD Biosciences, San Jose, CA). Data were analyzed using the BD FACStation™ Software (BD Biosciences, San Jose, CA). Quadrants were assigned using isotype control mAb. Data were processed using the CellQuest software.

Differentiation of bone marrow cells

Wild type FVB/N mouse femur bones were harvested and cut into small pieces aseptically to release bone marrow cells. The whole bone marrow cells were treated with 10 μM TTR/PMB for 2 days. The harvested cells were stained with antibodies against various cell surface markers, including CD11b, CD11c, F4/80, Ly6G and Ly6C, followed by intracellular staining of p-Akt, p-mTOR, pS6, p-NF-κB p65, p-ERK, and p-p38. The stained cells were subjective to flow cytometry analysis.

Reactive oxygen species (ROS) measurement of myeloid cells

Fresh bone marrow cells (1×10^6) from wild type mice were recovered in RPMI 1640 medium (10% FBS) at 37ºC for 1 hour, followed by treatment with or without TTR (1, 5 μM) in PMB (50 μg/ml) for 1 hour. Treated cells were stained with myeloid lineage specific surface markers and 2 μmol/L 2', 7'-dichlorofluorescein diacetate (Invitrogen). The ROS level was measured by flow cytometry in gated areas using a LSRII machine (Becton Dickinson).

Immunosuppressive assay of Ly6G$^+$ myeloid cells

Freshly isolated spleen CD4$^+$ T cells from the wild type mice were labeled with carboxyfluorescein diacetate succinimidyl diester (CFSE) and cultured in 96 wells plate (0.2×10^6 cells/ well), which were pre-coated with anti CD3 (2μg/ml in PBS) and anti CD28 (5μg/ml in PBS) antibodies in RPMI1640 medium (10% FBS) at 37ºC. Next day, freshly isolated Ly6G$^+$ cells from the bone marrow of wild type FVB/N mice that were treated with or without TTR (5 μM) overnight were added to CFSE-labeled CD4$^+$ T cells at a 5:1 ratio, and continuously incubated with or without 5 μM TTR in PMB (50 μg/ml) for 4 days. Cells were harvested and stained with APC-labeled anti-CD4 mAb (eBiosciences). Proliferation of CD4$^+$ T cells was evaluated as CFSE dilution by flow cytometry.

Endothelial cell (EC) tube formation:

ECs were isolated from the wild type lung as previously described (11), and treated with 50 μg/mL PMB, or 0.1 μM or 1 μM TTR/PMB for 24 h. Cells (5×10^4) were seeded in 48-well plates pre-coated with 150 μl/well growth factor-reduced matrigel (BD BioSiences). After 6 hours, tube formation was observed with an inverted microscope (Nikon, Melville, NY) as a tube-like structure exhibiting a length four times its width. Images of tube morphology were taken in 5 random microscopic fields per sample at × 40 magnifications, and the cumulative tube lengths were measured by Nikon NIS Elements imaging software.

EC migration

Wild type lung ECs (1.5×10^5) were seeded into a 24-well plate and incubated overnight to form a confluent monolayer. After creating a scratch on the cell monolayer, 50 μg/mL PMB, or 0.1μM or 1μM TTR/PMB was added into the medium in the presence of mitomycin C to prevent cell proliferation. Images were taken at 0 and 15 hours after creating the scratch. ECs migration was estimated by measuring the distance from one side of the scratch to the other side using Nikon NIS Elements imaging software.

Proliferation

Wild type lung ECs (5×10^4) were seeded into 24-well plates. Two days later, 50 μg/mL PMB, or 0.1μM or 1μM TTR/PMB was added into the medium. Twenty-four hours later, EC cell numbers were counted.

EC permeability

Isolated wild type lung ECs (5×10^4) were added to the upper chamber of 24-well 8.0-μm-pore Transwell plates (Corning, Tewksbury, MA). After incubated at 37°C, 5% CO_2 for 48

hours to form a monolayer, ECs were treated with 50 μg/mL PMB, or 0.1 μM or 1 μM TTR/PMB for 24 hours. The supernatant was removed, and CellTrackerTM Green 5-Chloromethylfluorescein Diacetate (CMFDA)-labeled bone marrow cells (1×10^4 cells in 200 μL media) were added to the upper well. Four hours later, transendothelial migration of bone marrow cells was determined by counting their numbers in the lower chamber from 5 randomly selected microscopic fields.

EC immunosuppression on T cells

The effect of TTR on wild type EC immunosuppressive function was analyzed by T cell proliferation assay. To isolate T cells, wild type mouse splenocytes were incubated with biotinylated anti-CD4 antibody, followed by positive selection on magnetic beads and eluted from magnetic separation columns according to the manufacturer's instructions (Miltenyi Biotec). The purified $CD4^+$ T cells were labeled with 1 μM carboxyfluorescein succinimidyl ester (CFSE) at 37°C for 10 min. After washing, cells were resuspended with growth medium and incubated at 37°C for 20 min. CFSE-labeled wild type $CD4^+$ T cells were co-cultured with ECs that were pre-treated with 50 μg/mL PMB, or 0.1 μM or 1 μM TTR/PMB in 96-well plates, which were pre-coated with anti-CD3 mAb and anti-CD28 mAb, for 4 days at 10:1 ratio between $CD4^+$ T cells: wild type ECs. The proliferation of $CD4^+$ T cells was analyzed by flow cytometry. PBS was used as a negative control.

Statistics

Statistical analyses were carried out in Word Excel 2016 (for animal studies) and SAS version 9.4 and R version 3.1.0 (for human studies). For animal studies, the data were mean values of multiple independent experiments and expressed as the mean ± SD. ANOVA and Tukey's method based on log-transformed concentration level were used to evaluate the significance of the differences. Statistical significance level was set at $p < 0.05$. For human serum analyses of biomarkers, Kruskal-Wallis tests with pair-wise Wilcoxon Rank Sum tests (Bonferroni-adjusted) were used to compare distributions of biomarkers among controls and cancer types. The area under the curve (AUC) was determined by cross-validated sensitivity-specificity ROC (Receiver Operating Characteristic) curve analysis to evaluate the diagnostic ability of biomarkers. To further distinguish between both cancer and controls and between different types of lung cancers, the CART method (Classification and Regression Tree – specifically RPART and TREE in R) was used. RPART utilizes all available cases. TREE, which only utilizes cases with all biomarkers available, was used to see if the classification results depended on the type of analytic method used.

Results

Stat3 downstream genes serve as biomarkers for human lung cancer diagnosis

The concentrations of all thirteen secretory proteins showed statistically significant differences in at least one type of lung cancer compared with normal human subjects by ELISA (Table 1). Optimal cut point for each biomarker using minimum specificity method (specificity=.80) and AUCs are listed in Table 1. When comparing central tendencies among the four groups, Markers 1, 2, 3, 4, 5, 6, and 10 all showed significant differences between each tumor type and control. For the other biomarkers, non-significant differences were seen

mostly in either squamous cells, small cells, or both. The areas under the ROCs display similar patterns. The lowest areas are for squamous cell and/or small cell in biomarkers 7–13. Statistical analyses using CART method (Classification and Regression Tree specifically RPART and TREE) revealed that different combinations in this panel of secretory protein biomarkers distinguished different types of lung cancers (Table 2). For example, the misclassification rate for cancer vs control was 11.2% using the RPART method.

The expression and distribution of TTR in CCSP-rtTA/$(TetO)_7$-Stat3C bitransgenic mice

Ups and downs of protein biomarkers in human patients implicate their functional roles in lung cancer formation. They are potential therapeutic targets for personalized lung cancer treatment if their pathogenic roles are clear. Based on its highly increased concentration and AUC in all three human lung cancer categories, TTR was chosen for further analysis. In addition to human lung cancers (Figure 1A, Table 1), TTR (monomer ~14 kDa) was detected in the sera of CCSP-rtTA/$(TetO)_7$-Stat3C bitransgenic mice. In doxycycline-treated bitransgenic mice with spontaneous lung tumors (CA group), all mice showed higher TTR protein levels (Figure 1B). In BALF from doxycycline-treated bitransgenic mice with spontaneous lung tumors, the TTR levels were also higher than those in BALF from other three groups (+DOX, -DOX and WT groups) (Supplemental Figure 1A). The intracellular TTR protein levels in the lung and blood were analyzed by flow cytometry analyses with anti-TTR antibody and cell surface markers. In the lung, the TTR expression levels were higher in whole lung cells, SPC^+ alveolar type II (AT II) epithelial cells, $CD11b^+Ly6G^+$ cells, and $Ly6G^+$ cells in doxycycline treatment (Figure 1C, Supplemental Figure 1B). In the blood, the TTR expression levels were also higher in whole white blood cells with doxycycline treatment, but not in $CD11b^+Ly6G^+$ cells, $CD11b^+$ cells and $Ly6G^+$ cells (Supplemental Figure 1C). The spleen showed no difference of TTR expression levels in doxycycline treated and untreated mice (Data not shown). By IHC staining of lung tissues, the TTR protein was positive in AT II epithelial cells (arrows) and alveolar macrophages in both doxycycline-treated and untreated bitransgenic mice, with stronger signals in the doxycycline-treated group (Figure 1D).

Recombinant TTR stimulates tumor cell proliferation and growth

TTR cDNA was subcloned and expressed in bacteria (supplemental Figure 2A-C). The purified recombinant TTR protein (1 or 5 μM) after LPS removal (supplemental Figure 2F) was incubated with Lewis lung carcinoma (LLC) cells or B16 melanoma cells for cell proliferation assessment in *in vitro* cell culture experiment. To eliminate the effect of residual LPS in recombinant TTR, polymyxin B (PMB) was used to block LPS. Comparing with the PMB control group, TTR treatment significantly enhanced LLC or B16 melanoma cell proliferation (Figure 2A). Recombinant TTR without LPS removal showed a similar result (Supplemental Figure 2G-H). In all subsequent studies, LPS-removed recombinant TTR was used in combination with PMB to minimize the LPS interference. In tumor growth *in vivo* study, LLC cells or B16 melanoma cells were pre-treated with recombinant TTR/PMB and flank-injected into syngeneic C57BL/6 mice. The flank-injected LLC tumors with TTR/PMB pre-treatment grew much faster than those with PMB treated control mice at 11, 14, and 18 days post injection (Figure 2B). In the allogeneic FVB/N mouse model, LLC tumors showed the same results, although the tumor sizes were smaller in general (Figure

2C). When the B16 melanoma model was tested, similar results were observed (Supplemental Figure 2I-J).

The levels of phosphorylated forms of mitogenic molecules Akt1, mTOR, S6, ERK, p38, NFκB p65, and Stat3 proteins were investigated by TTR/PMB treatment. TTR/PMB treatment of LLC cells led to increased activation of p-Akt1, p-mTOR, and p-NFκB p65, while the levels of p-ERK and p-p38 were relatively unchanged (Figure 2D). Inhibition of Akt1, mTOR or Akt1/mTOR by siRNAs knockdown (Supplemental Figure 2K) impaired LLC's proliferative ability in response to TTR/PMB treatment (Figure 2E). When tested in vivo, LLC cells were knocked down with Akt1, mTOR, or Akt1/mTOR siRNAs before subcutaneous flank-injection to the wild type C57BL/6 recipient mice. mTOR knockdown greatly decreased tumor growth by TTR/PMB stimulation comparing with control siRNA knockdown, which was further decreased by Akt1/mTOR double knockdown (Figure 2F). NFκB p65 knockdown (Supplemental Figure 2K) also decreased tumor growth by TTR/PMB stimulation comparing with control siRNA knockdown ($p<0.05$) (Figure 2G). These results suggest that the Akt1/mTOR pathway and the NFκB pathway in cancer cells are responsible for TTR stimulation.

TTR is an immune cell regulator

In addition to directly stimulating cancer cells, it is intriguing to determine if TTR is involved in differentiation of various immune cells that are known to play important roles in the tumor environment. Purified and LPS-removed recombinant TTR was injected into wild type mice twice in one week for two weeks. Profiling of total bone marrow cells by flow cytometry showed that the majority of immune cells in the myeloid compartment ($CD11b^+Ly6G^+$, $CD11b^+$, $Ly6G^+$, $Ly6C^+$, $F4/80^+$ cells) showed increased differentiation, while $CD8^+$ and $B220^+$ cells were decreased comparing with the control group (Figure 3A, Supplemental Figure 3A). This concludes that TTR has a cytokine-like function specific for increasing myeloid cell differentiation in the bone marrow.

To confirm these observations of myeloid differentiation, whole bone marrow cells were isolated from wild type mice and cultured *in vitro* with TTR/PMB for two days. TTR/PMB stimulated $CD11b^{high+}$, $CD11C^+$ and $F4/80^+$ myeloid lineage differentiation in a dose dependent manner (Figure 3C,D,F), while stimulated $Ly6C^{high+}$, MHCII myeloid lineage differentiation starting at a low dosage of TTR (0.2 μM) (Figure 3B,G). The $Ly6G^+$ population was the only exception, showing down-regulation (Figure 3E) that contradicts the *in vivo* observation (Figure 3A). The double positive $CD11b^{high+}Ly6C^{high+}$ cells, which are myeloid progenitor cells, were also increased in a dose-dependent manner after TTR/PMB treatment (Figure 3H). To show the activation status of immune cells treated by TTR/PMB, activation of various cellular signaling molecules were investigated. As demonstrated in Figure 4A-C (and Supplemental Figure 4A-C), the phosphorylation levels of Akt1, mTOR, and S6 were increased after TTR/PMB treatment by flow cytometry, suggesting that the metabolic reprogramming controlled by the Akt1/mTOR pathway is involved in TTR-mediated myeloid lineage differentiation. Activation of ERK, p38, and NFκB p65 molecules were also concomitantly increased in myeloid lineage cells (Figure 4D-F, and Supplemental Figure 4D-F).

TTR increases ROS production and immunosuppression of myeloid cells

Functionally, TTR/PMB treatment increased cellular ROS production in $CD11b^+$, $Ly6G^+$, $CD11b^+Ly6G^+$, $CD11C^+$, $Ly6C^+$, $MHCII^+$ and $F4/80^+$ myeloid lineage cells (Figure 5A, Supplemental Figure 3B). High level expression of ROS is a hallmark for the $CD11b^+Ly6G^+$ myeloid population to be immunosuppressive. This may explain why $CD8^+$ or $B220^+$ cell differentiation was suppressed after TTR/PMB *in vivo* treatment (Figure 3A). To confirm this assumption, *in vitro* CFSE-labeled T cell proliferation was performed by incubating with TTR/PMB treated $CD11b^+Ly6G^+$ cells. While TTR/PMB treatment alone showed no effect on T cell proliferation (Figure 5B, middle panel), TTR/PMB treatment of $CD11b^+Ly6G^+$ cells from the bone marrow showed significant suppression on CFSE-labeled wild type splenocyte T cell proliferation in co-culture experiment with stimulation of anti-CD3 mAb plus anti-CD28 mAb (Figure 5B, lower panel). It seems that TTR treatment is able to convert wild type bone marrow $CD11b^+Ly6G^+$ cells to myeloid-derived suppressive cells (MDSCs). Therefore, increased TTR concentration creates an immunosuppressive environment to benefit tumor growth.

TTR enhances EC angiogenic functions

Endothelial cells are major cellular component of the alveolar structure and pulmonary vasculature, which control infiltration of cancer cells and immune cells into the lung. As shown in Figure 6A, the TTR expression level was significantly increased in lung $CD31^+$ ECs after doxycycline treatment of CCSP-rtTA/$(TetO)_7$-Stat3C bitransgenic mice. To determine whether TTR influences the formation of capillary-like tubes by lung ECs, an important parameter of angiogenesis, the *in vitro* matrigel tube formation assay was performed. TTR/PMB pre-treated wild type ECs formed more tubes than those of PMB pre-treated control ECs, demonstrating that TTR had ability to enhance EC tube formation *in vitro* (Figure 6B). To test whether TTR/PMB affects EC migrating ability, monolayers of wild type ECs were treated with PMB or TTR/PMB in the presence of mitomycin C to eliminate the potential effects of EC proliferation. As shown in Figure 6C, 15 h after creating the scratch, TTR/PMB-treated wild type ECs demonstrated increased migration comparing with that of PMB-treated ECs in wound healing assay, evidenced by a significantly reduced wound area lacking cells. In a separate experiment, TTR/PMB stimulated EC proliferation (Figure 6D). Transwell assay was performed to determine the effect of TTR/PMB on the EC permeability. Freshly isolated wild type bone marrow cells were labeled with CMFDA and loaded on primary lung EC monolayers that were pre-treated with PMB or TTR/PMB for 24 h. As shown in the Figure 6E, TTR/PMB-treated wild type lung ECs showed increased permeability with more bone marrow cells migrating to the lower chamber than that of PMB-treated ECs. ECs are known for their influence on T cell activity (12). When wild type ECs were pre-treated with TTR/PMB and co-cultured with CFSE-labeled wild type splenocyte $CD4^+$ T cells, with stimulation of anti-CD3 mAb plus anti-CD28 mAb, TTR/PMB treated ECs suppressed T cell proliferation comparing with that of PMB-pretreated ECs (Figure 6F).

Discussion

Lung cancers are inflammation-associated diseases. Inflammatory molecules are valuable tools to reveal lung cancer occurrence. At the moment, the clinical solution for lung cancer detection using protein biomarkers is challenging and premature (13). This is because lung cancers are heterogeneous diseases and caused by multiple factors, a particular biomarker may or may not be up-regulated in a given patient. Conversely, a given biomarker can be upregulated in different types of diseases. Therefore, it is difficult to use one or two biomarkers for accurate lung cancer detection or prediction. To solve this clinical challenge, multiple biomarkers should be developed and used for more accurate lung cancer detection and classification. Different inflammatory diseases (including cancers) produce distinctive sets of molecules, which can be used as a panel of signature biomarkers for disease distinguishing. Since the high expression level of STAT3 was associated with advanced tumor stage (14), secretory protein biomarkers identified here have multiple advantages, especially they detect lung cancer in the patient blood without going through biopsy (Table 1). Combination of these biomarkers significantly eliminated false positive rate in lung cancer diagnosis. Importantly, they distinguished different types of human lung cancers (Table 2).

Upregulation of protein biomarkers contributes to the tumor microenvironment that in favor of tumor growth and metastasis. Therefore, it is critical to elucidate their functional roles in tumor formation and immune reaction in order to better use them for lung cancer prediction, and further, for personalized treatment and precision medicine. Previously, chitinase 3-like 1 (CHI3L1), one of 13 biomarkers, has been shown to stimulate proliferation and growth of lung cancer cells (9). TTR was originally identified as a transport protein in the serum that carries the thyroid hormone thyroxine (T_4) and retinol-binding protein bound to retinol (6, 15). It has been extensively studied in the brain, and associated with neurological diseases (16). In this report, TTR was highly expressed in the blood of human patients with adenocarcinoma, squamous carcinoma and small cell lung cancer (Figure 1A). The same observation was confirmed in the CCSP-rtTA/$(tetO)_7$-Stat3C lung tumor mouse model (Figure 1B), which matched the result of gene profile analysis (2). In addition to being produced by alveolar type II epithelial cells where Stat3C was overexpressed, TTR was also produced by pulmonary myeloid lineage cells (Figure 1C, D) and lung endothelial cells (Figure 6A) in the CCSP-rtTA/$(tetO)_7$-Stat3C mouse model, probably through secondary inducible effects.

Based on our characterization, TTR has pleiotropic functions in multi-aspects of tumorigenesis. First, TTR directly targeted and stimulated LLC and B16 melanoma cell proliferation *in vitro* and growth *in vivo* (Figure 2A-C, Supplemental Figure 2G-J). This was mediated through activation of the Akt/mTOR and NFκB pathways (Figure 2D). mTOR is a master regulator of serine/threonine protein kinase family member that regulates cell growth, proliferation, migration, survival, protein synthesis and transcription in response to growth factors and mitogens (17). Oncogenic activation of the mTOR pathway has been reported to induce several processes required for cancer cell growth, survival and proliferation (18). Akt1 is the upstream regulator of mTOR. Ablation of Akt1 and mTOR by siRNA knockdown reduced TTR stimulation of LLC proliferation and growth (Figure 2E-F). These

observations showed that metabolic master regulator mTOR is required for TTR stimulation of tumor cells. NFκB is another important oncogenic pathway important for tumor growth (19). Ablation of NFκB by siRNA knockdown reduced TTR stimulation of LLC tumor growth as well (Figure 2G).

Second, in addition to directly stimulating cancer cell proliferation and growth, TTR demonstrated features of cytokines to regulate immune cell differentiation. Tumor initiation, growth and metastasis are largely facilitated and dependent on their interactions with surrounding immune cells, which are critical components in the tumor environment. The high levels of TTR in the blood of human lung cancer patients and the CCSP-rtTA/$(tetO)_7$-Stat3C lung tumor animal model inevitably influence immune cell development and functions. Indeed, TTR injection into wild type mice led to increased differentiation of myeloid lineage cells ($CD11b^+Ly6G^+$, $CD11b^+$, $Ly6G^+$, $Ly6C^+$, $F4/80^+$), and decreased $CD8^+$ and $B220^+$ cells (Figure 3A). This was confirmed by *in vitro* study in which TTR stimulated myeloid lineage differentiation of isolated wild type bone marrow cells (Figure 3B-H). Similar to cancer cells, TTR activated Akt1, mTOR, and S6 phosphorylation in myeloid lineage cells (Figure 4A-C). This is consistent with previous observations that mTOR-mediated metabolic reprogramming plays a critical role in myeloid-mediated tumor immunity (20, 21). ERK, p38, and NFκB p65 were also activated by TTR in myeloid cells (Figure 4D-F). In a separate mechanism, overproduction of ROS in myeloid lineage cells plays a critical role in their pro-tumor activity. Not only TTR treatment stimulated ROS production in wild type myeloid cells, but also converted wild type bone marrow $CD11b^+Ly6G^+$ cells to become MDSCs that suppressed splenocyte T cell proliferation (Figure 5). Anti-tumor rejection largely relies on proper T cell proliferation and functions.

Third, the increased TTR concentration in the circulation system influences angiogenesis and EC functions. ECs are the major component of blood vessels and actively participate in regulation of inflammatory and tumorigenic processes through controlling circulating cell migration, vessel permeability, and cell infiltration into organs (22). TTR regulated ECs functions in several folds. It had ability to influence angiogenesis by enhancing EC tube formation (Figure 6B), and stimulating EC proliferation (Figure 6D). Permeability of EC depends on angiogenesis. TTR showed ability to increase both EC migration (Figure 6C) and permeability (Figure 6E). Migration, penetration and function of leucocytes and cancer cells in the blood are influenced by ECs. TTR treated ECs showed suppression of T cell proliferation (Figure 6F). It is noted that TTR showed modest effects on some cell types. However, combination of these effects contribute enormously to stimulation of tumor growth *in vivo* by surged TTR (Figure 2B&C, Supplemental Figure 2I&J), and created an immunosuppressive environment to benefit tumor growth.

Taken together, Stat3 and its downstream inducible protein biomarkers show promise as a valuable tool for lung cancer detection and classification. These blood soluble biomarkers actively participate in tumor proliferation, growth and invasion by directly stimulating cancer cells, as well as regulating immune cells and ECs in the tumor environment. Therefore, these biomarkers have potential for use as clinical targets for lung cancer personalized treatment if their expression levels are increased in a given lung cancer patient in the blood.

Supplementary Material

Refer to Web version on PubMed Central for supplementary material.

Acknowledgment

We thank Mr. Haijiao Xu for statistical analysis.

This work was supported by National Institutes of Health Grants CA138759, CA152099 (to C. Y.), and HL087001 (to H. D.), and grants from Dean's office of Indiana University School Medicine.

Abbreviations used in this article:

AUC	the area under the curve
BALF	bronchoalveolar lavage fluid
CHI3L1	chitinase 3-like 1
CMFDA	5-Chloromethylfluorescein Diacetate
ECs	endothelial cells
FACS	fluorescence activated cell sorting
HRP	horseradish peroxidase
LLC	Lewis lung carcinoma
PMB	polymyxin B
ROC	Receiver Operating Characteristic
Stat3	signal transducer and activator of transcription 3
TTR	transthyretin
MDSCs	myeloid-derived suppressive cells
ROS	Reactive oxygen species

References

1. Rami-Porta R, Ball D, Crowley J, Giroux DJ, Jett J, Travis WD, Tsuboi M, Vallieres E, Goldstraw P, International Staging C, Cancer R, Biostatistics C Observers to the, and I. Participating. 2007 The IASLC Lung Cancer Staging Project: proposals for the revision of the T descriptors in the forthcoming (seventh) edition of the TNM classification for lung cancer. J Thorac Oncol 2: 593–602. [PubMed: 17607114]
2. Li Y, Du H, Qin Y, Roberts J, Cummings OW, and Yan C 2007 Activation of the signal transducers and activators of the transcription 3 pathway in alveolar epithelial cells induces inflammation and adenocarcinomas in mouse lung. Cancer Res 67: 8494–8503. [PubMed: 17875688]
3. Yu H, Lee H, Herrmann A, Buettner R, and Jove R 2014 Revisiting STAT3 signalling in cancer: new and unexpected biological functions. Nat Rev Cancer 14: 736–746. [PubMed: 25342631]
4. Harada D, Takigawa N, and Kiura K 2014 The Role of STAT3 in Non-Small Cell Lung Cancer. Cancers (Basel) 6: 708–722. [PubMed: 24675568]

5. Qu P, Roberts J, Li Y, Albrecht M, Cummings OW, Eble JN, Du H, and Yan C 2009 Stat3 downstream genes serve as biomarkers in human lung carcinomas and chronic obstructive pulmonary disease. Lung Cancer 63: 341–347. [PubMed: 18614255]
6. Lim A, Sengupta S, McComb ME, Theberge R, Wilson WG, Costello CE, and Jacobsen DW 2003 In vitro and in vivo interactions of homocysteine with human plasma transthyretin. J Biol Chem 278: 49707–49713. [PubMed: 14507924]
7. Episkopou V, Maeda S, Nishiguchi S, Shimada K, Gaitanaris GA, Gottesman ME, and Robertson EJ 1993 Disruption of the transthyretin gene results in mice with depressed levels of plasma retinol and thyroid hormone. Proc Natl Acad Sci U S A 90: 2375–2379. [PubMed: 8384721]
8. van Bennekum AM, Wei S, Gamble MV, Vogel S, Piantedosi R, Gottesman M, Episkopou V, and Blaner WS 2001 Biochemical basis for depressed serum retinol levels in transthyretin-deficient mice. J Biol Chem 276: 1107–1113. [PubMed: 11036082]
9. Yan C, Ding X, Wu L, Yu M, Qu P, and Du H 2013 Stat3 downstream gene product chitinase 3-like 1 is a potential biomarker of inflammation-induced lung cancer in multiple mouse lung tumor models and humans. PLoS One 8: e61984. [PubMed: 23613996]
10. Li Y, Qu P, Wu L, Li B, Du H, and Yan C 2011 Api6/AIM/Spalpha/CD5L overexpression in alveolar type II epithelial cells induces spontaneous lung adenocarcinoma. Cancer Res 71: 5488–5499. [PubMed: 21697282]
11. Zhao T, Ding X, Du H, and Yan C 2014 Myeloid-derived suppressor cells are involved in lysosomal acid lipase deficiency-induced endothelial cell dysfunctions. J Immunol 193: 1942–1953. [PubMed: 25000979]
12. Carman CV, and Martinelli R 2015 T Lymphocyte-Endothelial Interactions: Emerging Understanding of Trafficking and Antigen-Specific Immunity. Frontiers in immunology 6: 603. [PubMed: 26635815]
13. Vargas AJ, and Harris CC 2016 Biomarker development in the precision medicine era: lung cancer as a case study. Nat Rev Cancer 16: 525–537. [PubMed: 27388699]
14. Wu P, Wu D, Zhao L, Huang L, Shen G, Huang J, and Chai Y 2016 Prognostic role of STAT3 in solid tumors: a systematic review and meta-analysis. Oncotarget 7: 19863–19883. [PubMed: 26959884]
15. Vieira M, and Saraiva MJ 2014 Transthyretin: a multifaceted protein. Biomol Concepts 5: 45–54. [PubMed: 25372741]
16. Alshehri B, D'Souza DG, Lee JY, Petratos S, and Richardson SJ 2015 The diversity of mechanisms influenced by transthyretin in neurobiology: development, disease and endocrine disruption. Journal of neuroendocrinology 27: 303–323. [PubMed: 25737004]
17. Guertin DA, and Sabatini DM 2007 Defining the role of mTOR in cancer. Cancer Cell 12: 9–22. [PubMed: 17613433]
18. Laplante M, and Sabatini DM 2012 mTOR signaling in growth control and disease. Cell 149: 274–293. [PubMed: 22500797]
19. Taniguchi K, and Karin M 2018 NF-kappaB, inflammation, immunity and cancer: coming of age. Nat Rev Immunol 18: 309–324. [PubMed: 29379212]
20. Ding X, Du H, Yoder MC, and Yan C 2014 Critical Role of the mTOR Pathway in Development and Function of Myeloid-Derived Suppressor Cells in lal(−/−) Mice. Am J Pathol 184: 397–408. [PubMed: 24287405]
21. Zhao T, Du H, Ding X, Walls K, and Yan C 2015 Activation of mTOR pathway in myeloid-derived suppressor cells stimulates cancer cell proliferation and metastasis in lal(−/−) mice. Oncogene 34: 1938–1948. [PubMed: 24882582]
22. Pober JS, and Sessa WC 2007 Evolving functions of endothelial cells in inflammation. Nat Rev Immunol 7: 803–815. [PubMed: 17893694]

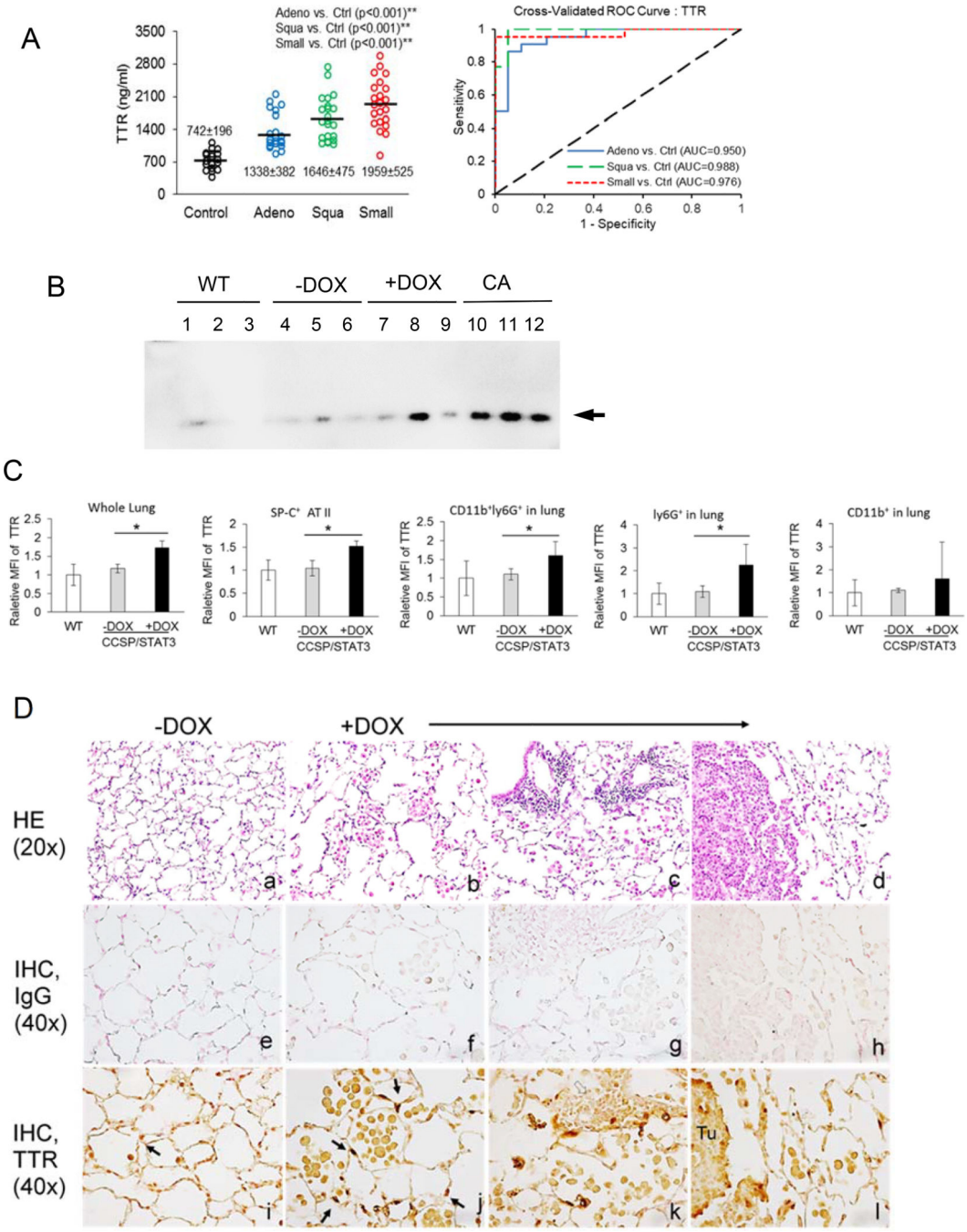

Figure 1. Expression and distribution of TTR in humans and CCSP-rtTA/(TetO)$_7$- Stat3C bitransgenic mice.

(**A**) Concentrations of TTR were determined by ELISA and cross-validated receiver operating characteristic (ROC) curve in human serum of normal smoker without cancer (control), adenocarcinoma (Adeno), squamous carcinoma (Squa) and small cell lung cancer (Small). ELISA results of other secretory protein biomarkers are summarized in Table 1; (**B**) The expression levels of TTR in the plasma of CCSP-rtTA/(TetO)$_7$-Stat3C bitransgenic mice were determined by Western blot. The arrow points to TTR. WT, wild type; -Dox,

doxycycline untreated; +Dox, doxycycline treated without tumor; CA, doxycycline treated with tumor; (**C**) The relative TTR expression levels in whole cells, SPC^+ cells, $CD11b^+Ly6G^+$ cells, $Ly6G^+$ cells and $CD11b^+$ cells of the lungs from WT and doxycycline treated (+DOX) and untreated (-DOX) CCSP-rtTA/$(TetO)_7$-Stat3C bitransgenic mice were determined by flow cytometry. n=4. *, $p<0.05$. See gating strategies in Supplemental Figure 1B; (**D**) Hematoxylin-eosin (HE) staining (a-d) and immunohistochemical (IHC) staining against TTR (e-l) in the lungs of bitransgenic mice with (+DOX) or without (-DOX) doxycycline treatment. Solid arrows: alveolar type II epithelial cells. Nonsolid arrow: perivascular infiltrated immune cells. Tu: tumor. Original magnification: 200× (for H & E) and 400× (for IHC).

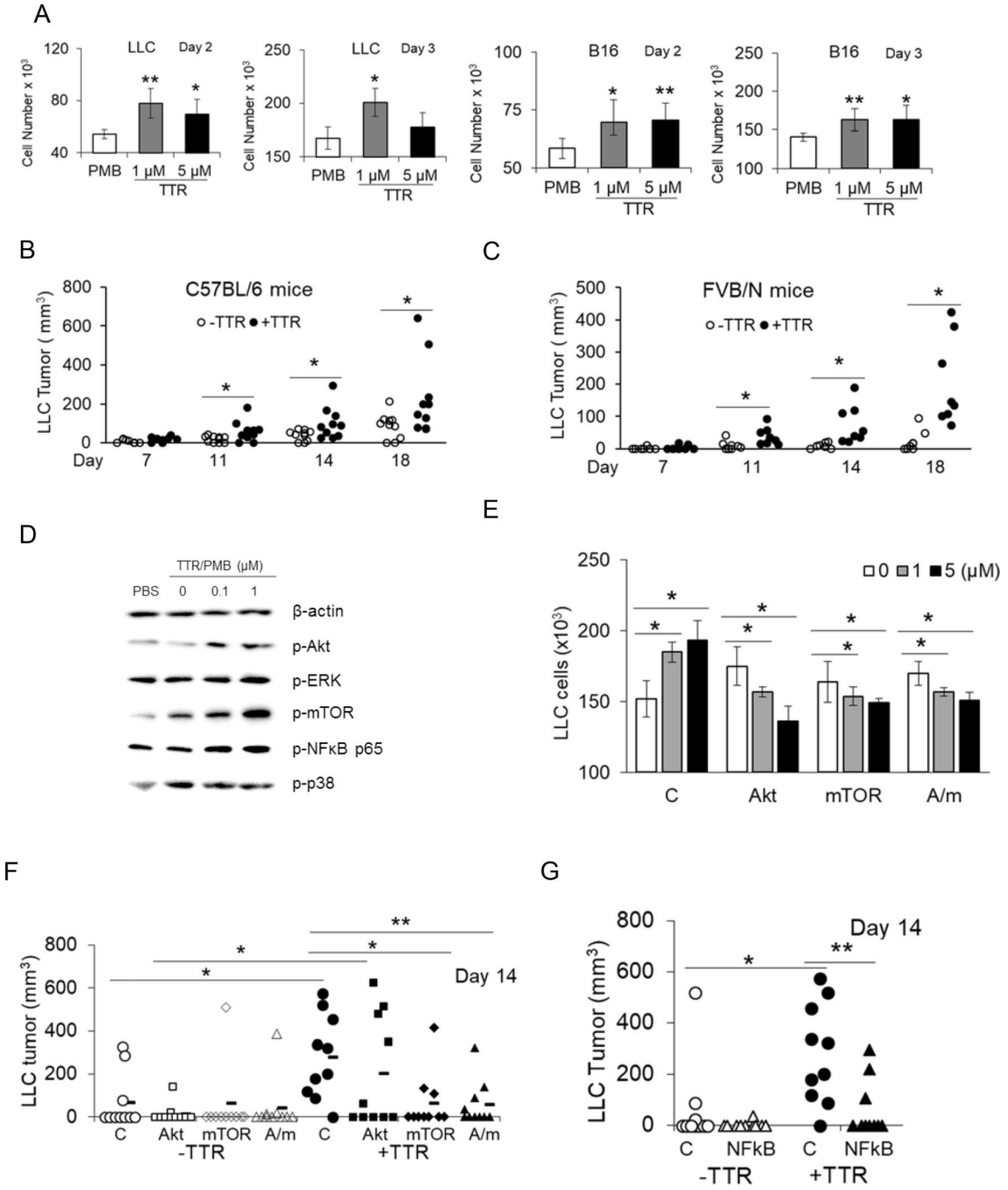

Figure 2. Recombinant TTR stimulates tumor in vitro proliferation and in vivo growth.

(**A**) Lewis lung carcinoma (LLC) cells or B16 melanoma cells were treated with 0, 1 or 5 μM TTR in the presence of polymyxin B (PMB). Cell numbers were determined by trypan blue exclusion assay. n=4–5, *, $p<0.05$, **, $p<0.01$; (**B**) LLC cells (5×10^5) were pre-treated with PBS (-TTR) or 20 μM TTR (+TTR) and flank injected in wild-type syngeneic recipient C57BL/6 mice. n=10, *, $p<0.05$, **, $p<0.01$; (**C**) LLC cells (5×10^5) were pre-treated with PBS (-TTR) or 20 μM TTR (+TTR) and flank injected in wild-type allogeneic recipient FVB/N mice. n=8, *, $p<0.05$, **, $p<0.01$; (**D**) LLC cells were treated with 0, 0.1 or 1 μM

TTR in the presence of 100 μg/mL polymyxin B (PMB) for 2 hrs. The phosphorylation levels of p-Akt, p-ERK, p-mTOR, p-NF-κB p65, and p-p38 were determined by Western blot. β-actin was used as a loading control; (**E**) Cell numbers (proliferation) of 0, 1, or 5 μM TTR-treated LLC cells were determined with Akt, mTOR or Akt/mTOR (A/m) knockdown by siRNAs for 2 days. n=4, *, $p<0.05$; (**F**) Tumor volumes in syngeneic recipient C57BL/6 mice 14 days after flank injection of Akt, mTOR or Akt/mTOR (A/m) siRNA knockdown-LLC cells (5×10^5 cells) that were pre-treated with 5 μM TTR. n=10, *, $p<0.05$, **, $p<0.01$; (**G**) Tumor volumes in syngeneic recipient C57BL/6 mice 14 days after flank injection of NFκB p65 siRNA knockdown-LLC cells (5×10^5 cells) that were pre-treated with 5 μM TTR. n=10, *, $p<0.05$, **, $p<0.01$. The tumor growth was measured by the maximal length (L) and width (W) and the tumor volume was calculated by the formula: $LxW^2/2$ (mm^3).

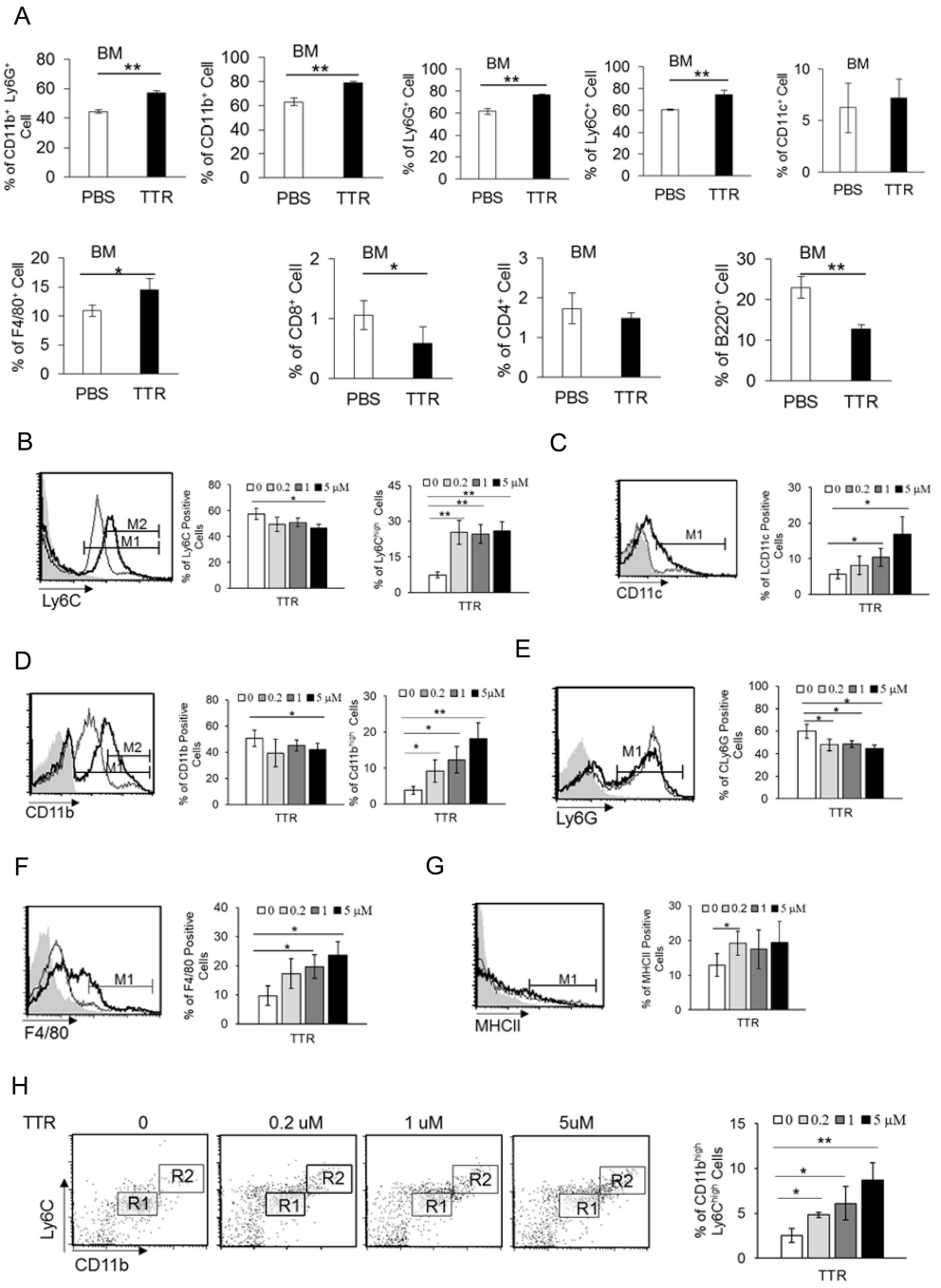

Figure 3. Recombinant TTR stimulates immune cell differentiation in the bone marrow.

(A) The TTR effect on differentiation of bone marrow lineage cells *in vivo*. TTR (320 μg / mouse) was i.v. injected into wild type mice twice a week for two weeks, and PBS was used as control. Single cells from the bone marrow were analyzed by flow cytometry. The percentage numbers of various immune cells were presented. See gating strategies in Supplemental Figure 3A. (B-H) The TTR effect on differentiation of bone marrow myeloid lineage cells *in vitro*. Whole bone marrow cells were isolated from wild type mice and cultured *in vitro* with 0, 0.2, 1, or 5 μM TTR for two days. The percentage numbers of

various immune cells after flow cytometry and statistical analysis were presented. Results are mean ± SD from four mice in each group (n = 4). In all above, *, $p<0.05$. **, $p<0.01$.

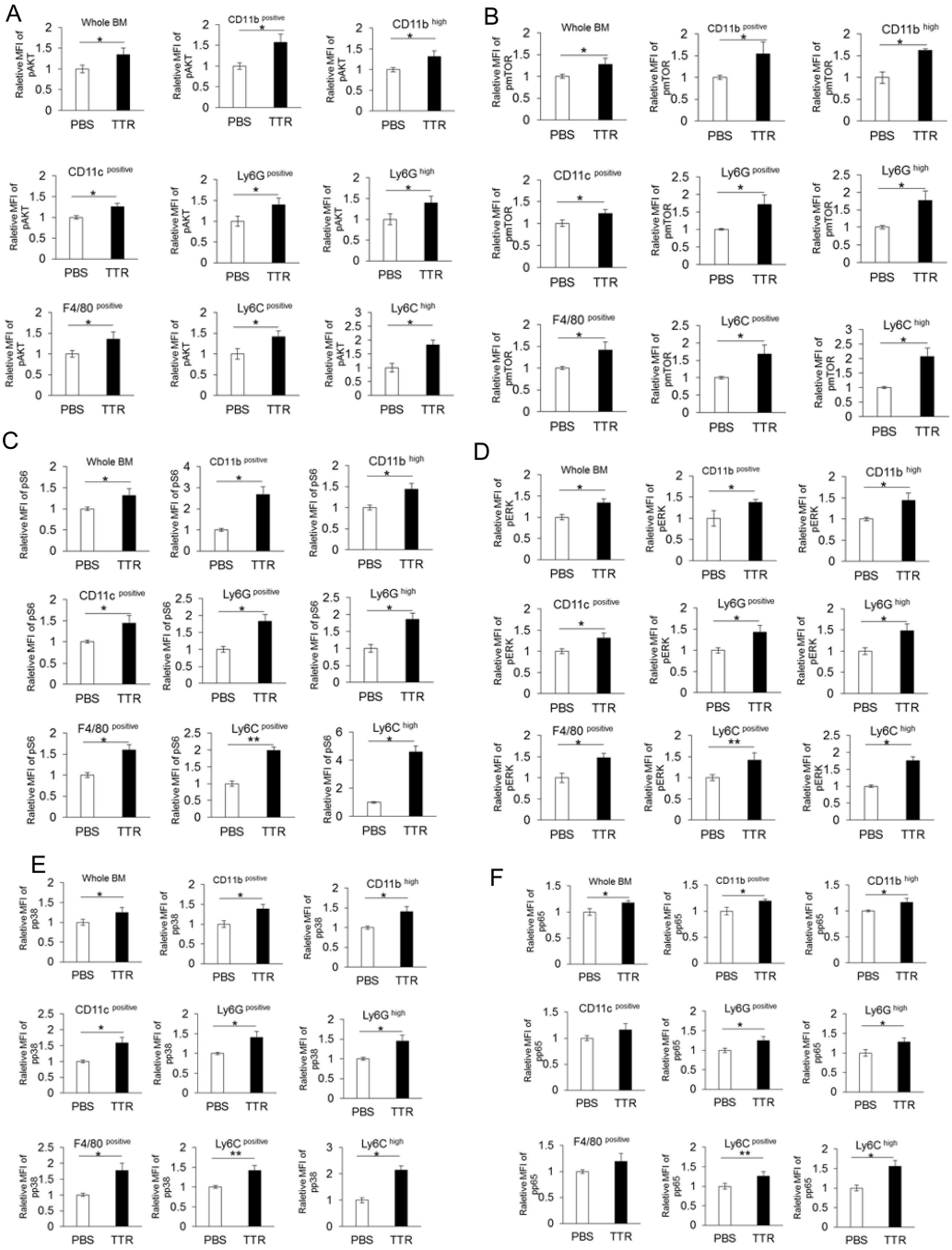

Figure 4. Stimulation of signaling molecules involved in differentiation of bone marrow myeloid lineage.

(**A-F**) Whole bone marrow cells were isolated from wild type mice and cultured *in vitro* with TTR (5 μM) treatment for 2 days. Antibodies against phosphorylated Akt, mTOR, S6, ERK, p38, and NFκB p65 in myeloid lineage cells were used, gated and analyzed by flow cytometry. The mean fluorescent intensity (MFI) were presented. Results are mean ± SD, n = 4, *, $p < 0.05$. **, $p < 0.01$. See gating strategies in Supplemental Figure 4.

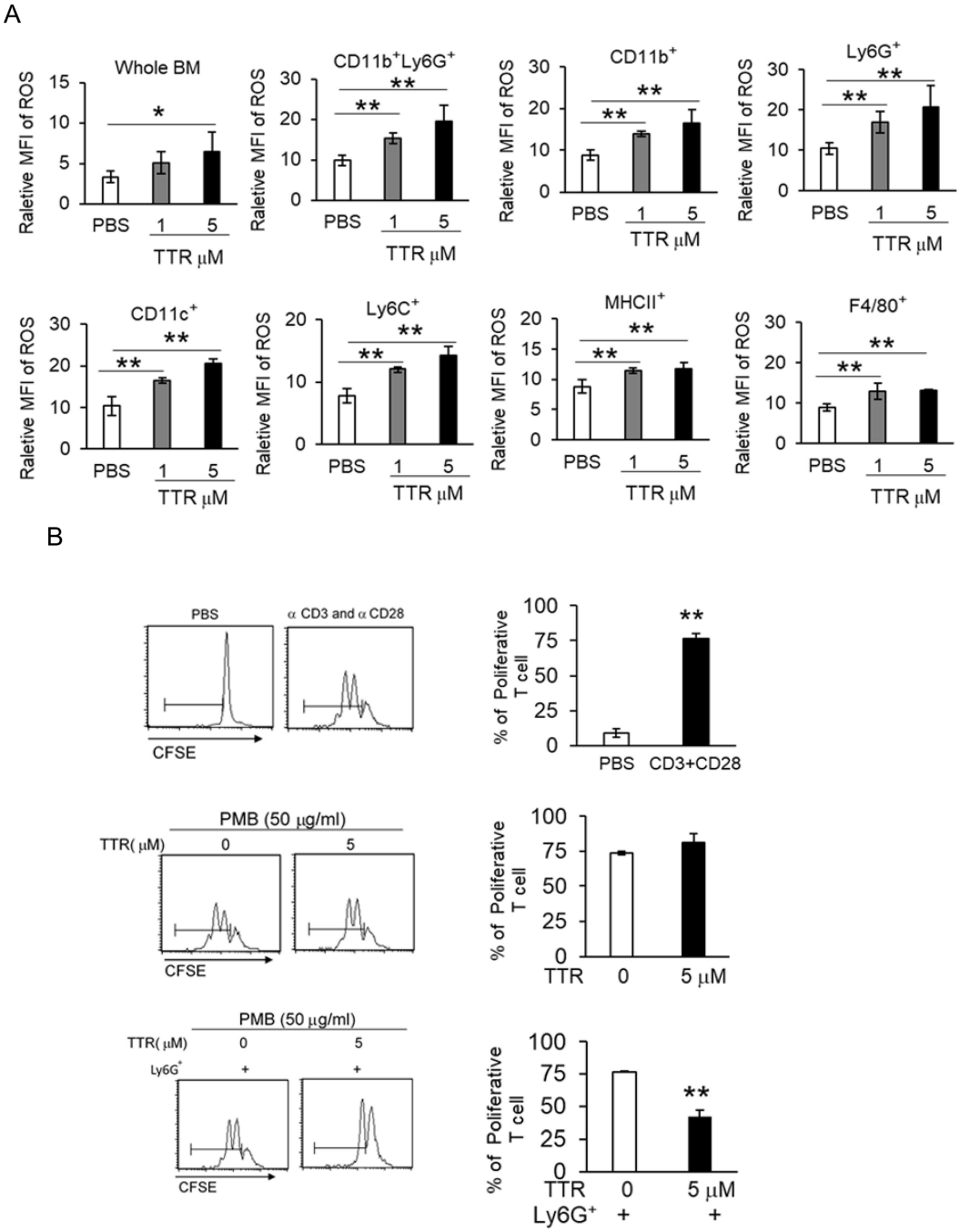

Figure 5. TTR increases ROS production and immunosuppression of myeloid cells.

(A) ROS production in gated myeloid cells. n=4. *, p<0.05. **, p<0.01. See gating strategies in Supplemental Figure 3B. (**B**) Immunosuppressive assays of Ly6G$^+$ cells. CD4$^+$ T cells were labeled with CFSE and stimulated by anti-CD3 and anti-CD28 antibodies (upper panel). TTR/PMB treatment alone did not affect splenocyte T cell proliferation (middle panel). TTR (5 μM) treated bone marrow Ly6G$^+$ cells showed suppression on splenocyte T cell proliferation (lower panel). n=4. *, p<0.05. **, p<0.01.

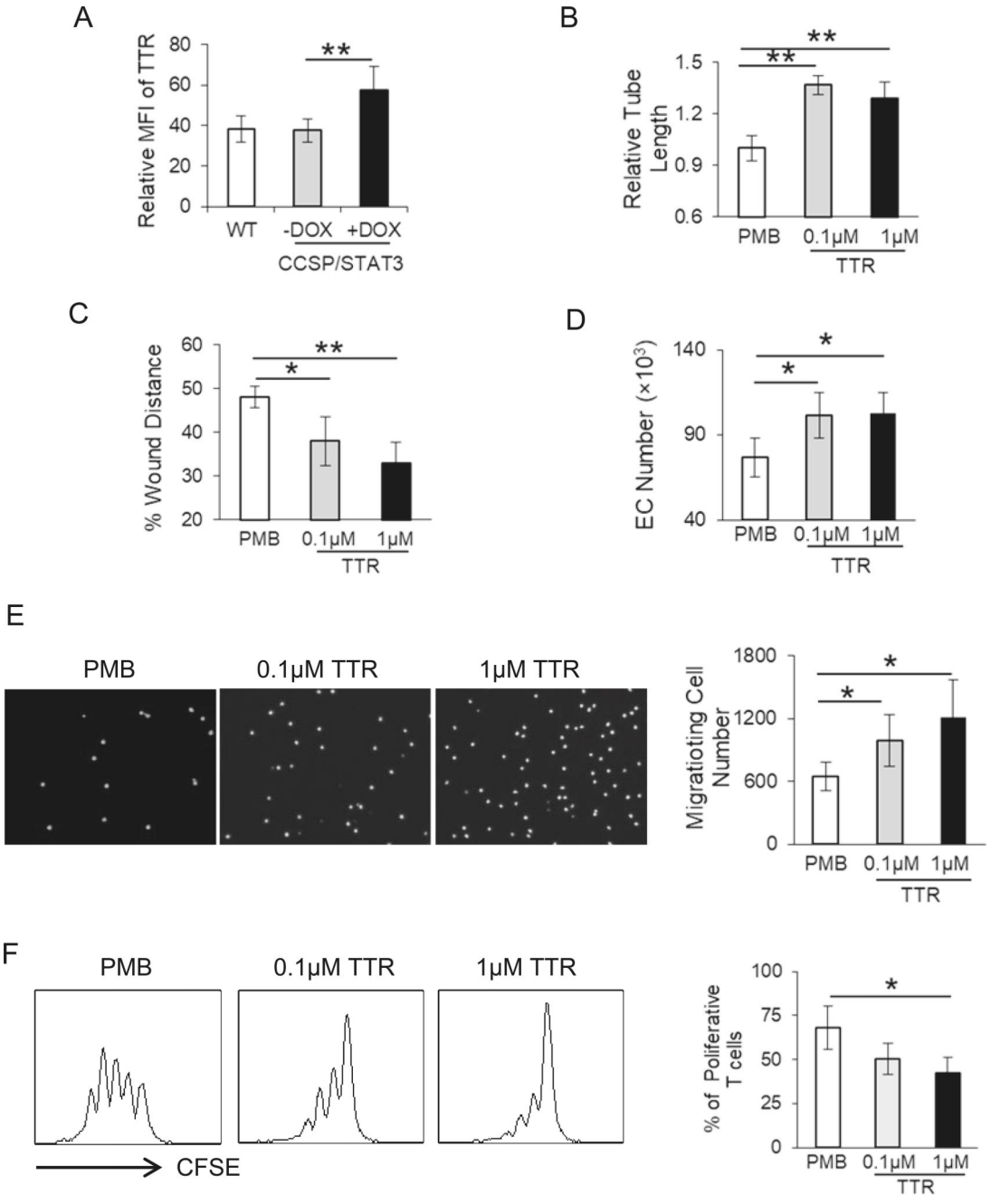

Figure 6. TTR enhances EC angiogenic functions in the lung.

(**A**) TTR expression in ECs was measured by gating $CD31^+$ cells in whole lung cells of doxycycline-treated (+DOX) or untreated (-DOX) CCSP-rtTA/$(TetO)_7$-Stat3C bitransgenic mice by flow cytometry. Wild type mice were used as control; (**B**) The effect of TTR on EC's *in vitro* tube formation was analyzed by matrigel tube formation assay. Wild type ECs from the lung were pre-treated with TTR or PMB for 24 hours and tube formation on matrigel were measured. Data were normalized to ECs treated with 50 μg/mL PMB; (**C**) The effect of TTR on EC migration was assessed by the *in vitro* wound healing assay in the presence of mitomycin C; (**D**) The effect of TTR on EC proliferation was assessed by

counting the cell number; (**E**) The effect of TTR on EC permeability was assessed by the *in vitro* trans-well assay. Fluorescence-labeled bone marrow cells were seeded onto the EC monolayer that was pre-treated with PMB or TTR. Bone marrow cells that migrated to the lower chamber were counted. Original magnification ×40. (**F**) TTR induced EC immunosuppression on T cells. CFSE-labeled wild type $CD4^+$ T cells were co-cultured with PMB or TTR pre-treated ECs and stimulated by anti-CD3 mAb and anti-CD28 mAb, followed by flow cytometry analysis. Peaks represent cell division cycles. PBS was used as a negative control. In all above experiments, data were expressed as mean ± SD; n = 4–5. *P < 0.05, **P < 0.01.

Table 1.

Cross-Validated Area Under the ROC of 13 secretory protein biomarkers.

	Distribution Shift vs Control Group p-value*			Cross-Validated Area Under the ROC (cutpoint**)		
	Adenocarcinoma(n=29)	**Squamous Cell (n=30)**	**Small Cell (n=28)**	**Adenocarcinoma (n=29)**	**Squamous Cell (n=30)**	**Small Cell (n=28)**
Marker 1	<0.001	<0.001	0.001	.83 (30.4)	.87 (28.1)	.80 (27.5)
Marker 2	<0.001	<0.001	<0.001	.95 (742.0)	.988 (1646.0)	.98 (1959.0)
Marker 3	<0.001	<0.001	0.001	.998 (52.7)	.97(47.1)	.84 (45.8)
Marker 4	<0.001	<0.001	0.005	.98 (1441.3)	.99 (995.0)	.79 (759.5)
Marker 5	<0.001	<0.001	<0.001	1.0 (195.4)	.99 (130.2)	.89 (102.4)
Marker 6	<0.001	0.017	<0.001	1.0 (22.8)	.78 (22.2)	.96 (22.3)
Marker 7	0.009	0.049	1.000	.78 (29.0)	.72 (36.6)	.56 (33.9)
Marker 8	0.002	0.070	1.000	.82 (5.7)	.71 (6.3)	.58 (9.0)
Marker 9	0.143	0.029	0.421	.68 (21.4)	.74 (33.8)	.63 (32.1)
Marker 10	<0.001	0.001	<0.001	.89 (71.2)	.86 (72.3)	.93 (71.8)
Marker 11	<0.001	0.509	1.000	.88 (628.7)	.62 (655.4)	.52 (664.6)
Marker 12	0.310	0.188	0.044	.74 (4.3)	.67 (4.0)	.73 (4.1)
Marker 13	<.001	0.052	0.003	1.0 (18.5)	.72 (24.5)	.82 (18.5)

*All overall tests were significant at the .05 level. P-values for pair-wise Wilcoxon Rank Sum tests are Bonferroni-adjusted.

**Optimal cutpoint using minimum specificity method (specificity=.80).

Control group: normal human subjects without cancer. N = 29.

Secretory biomarker protein concentrations in human serum (50–100 μl) were determined by enzyme-linked immunoabsorbent assay (*ELISA*) according to the manufacturer's instruction (R&D Systems, Minneapolis, MN) (for each cancer group, n=28–30). The human serum samples were diluted to 1:100 before assay. The cross-validated area under the curve (AUC) was determined by sensitivity-specificity ROC (Receiver Operating Characteristic) curve analysis.

Marker 1: CHI3L 1 - Chitinase 3-like 1; Marker 2: TTR - Transthyretin; Marker 3: FGb - Fibrinogen, beta polypeptide; Marker 4: FGL 1 - Fibrinogen-like protein 1; Marker 5: GUCA2A - Guanylate cyclase activator 2A (guanylin); Marker 6: DLK1 - Delta-like 1 homolog (Drosophila); Marker 7: GLUT3 - Glucose Transporter 3; Marker 8: CBLN1 - Cerebellin 1; Marker 9: ELA 1 - Elastase 1, pancreatic; Marker 10: Fga - Fibrinogen, alpha polypeptide; Marker 11: HRG - Histidine-rich glycoprotein; Marker 12: SHH - Sonic hedgehog homolog; Marker 13: TMEM27 - Transmembrane protein 27.

Table 2.

Statistical analyses of the panel of secretory protein biomarkers in Table 1 using the CART method (Classification and Regression Tree - specifically RPART and TREE) to distinguish different types of lung cancers.

	n	#correctly classified	#misclassified	Error rate for RPART	Markers using Tree	Error Rate for TREE
Cancer vs Control						
2 splits-Marker 2 and Marker 3					M5, 9, 2	
Cancer	87	81	6			
Control	29	22	7			
	116	103	13	11.2%		4.2%
Adeno vs Control						
1 split-Marker 5					M3	
Adenocarcinoma	29	29	0			
Control	29	22	7			
	58	51	7	12.1%		0.0%
Small Cell vs Control						
1 split-Marker 2					M2 and 7	
Small Cell	28	27	1			
Control	29	19	10			
	57	36	11	19.3%		2.7%
Squamous Cell vs Control						
1 split - Marker 2					M5	
Squamous Cell	30	26	4			
Control	29	26	3			
	59	52	7	11.9%		0%
Using all 4 groups						
4 splits - Markers 2, 3, 13, 10					M3, 2, 13, 6, 7, 5	
Adenocarcinoma	29	23	6 (as 2 ctl, 4 sm)			
Control	29	22	7 (as 1 adeno, 6 sm)			
Small Cell	28	18	10 (as 6 adeno, 3 ctl, 1 sq)			
Squamous Cell	30	13	17 (as 10 adeno, 3 ctl, 4 sm)			
	116	76	40	34.5%		14.1%
Cancer Only						
5 splits - Markers 3, 13, 4, 12, 1					M3, 4, 13, 6	
Adenocarcinoma	29	25	4 (4 sq)			
Small Cell	28	20	8 (7 adeno, 1 sq)			
Squamous Cell	30	21	9 (8 adeno, 1 sm)			

	n	#correctly classified	#misclassified	Error rate for RPART	Markers using Tree	Error Rate for TREE
	87	66	21	24.1%		16.1%

For the RPART method, Markers 2 and 3 were chosen to distinguish between cancer and control (misclassification = 11.2%). When looking within the cancer samples only, Marker 3, 13, 4, 12 and 1 were chosen to classify the cancer types (misclassification rate = 24.1%). RPART utilizes all available data. For the TREE method, only cases with no missing biomarkers are used (n=71 out of 116 possible = 61%). Relevant markers are shown. Similar markers arise with both methods although Marker 5 comes up more often in the TREE method than RPART. The error rates are much lower with the TREE method, however 39% of the data is omitted. There were no differences in age, sex, or race between those with complete data and those who had a least one missing marker value.